

Thermal stabilization of chemical reactors. II. Bifurcation analysis of the Endex CSTR

R. Ball*

School of Chemistry, Macquarie University, NSW 2109 Australia

B.F. Gray†

School of Mathematics and Statistics,
University of Sydney, NSW 2006 Australia

Abstract

The steady states of the dynamical Endex CSTR problem are analysed in terms of degenerate bifurcation (singularity) theory. Steady-state analysis is used in two ways: (1) as a device to assist in understanding and predicting complex *dynamical* behaviour, and (2) as a practical design and operational tool, by applying the concept of quasi-static parameter variation. In the bifurcation analysis, consideration is given to the effects of thermal mismatching, kinetic mismatching, and variations in the thermal exchange, mass flux, and heat loss rate parameters, on the structure of the parameter space. The qualitative equivalence of the bifurcation structure of the kinetically matched, perfectly coupled adiabatic Endex scheme and the single-reaction adiabatic CSTR is demonstrated, with reference to the role of the reaction enthalpy effects. Numerical analysis shows that either kinetic mismatching of the reactions or imperfect heat exchange may introduce Hopf bifurcations into the adiabatic system. This is a result that is both philosophically and practically important because it shows that limit cycles are not restricted to non-adiabatic thermokinetic systems. The coefficients of thermal exchange, mass flux, and heat loss are found to induce distortions of the surface of saddle-node bifurcations (the limit-point shell) through codimension 2 bifurcations. The steady-state and oscillatory-state degeneracies are discussed with reference to the design and operational implications for a working system.

Keywords: Endex; bifurcation theory; singularity theory; thermokinetics; reactive thermal coupling; limit-point shell

*Corresponding author. Present address: Department of Theoretical Physics, Research School of Phys. Sci. & Eng. ANU, Canberra ACT 0200 Australia E-mail: rxb105@rsphysse.anu.edu.au

†Present address: School of Chemistry, Macquarie University, NSW 2109 Australia. E-mail: bgray@laurel.ocs.mq.edu.au

1 Introduction

In a previous paper (Gray & Ball (1999), hereafter referred to as Part I), we presented an exposition of the Endex CSTR as a dynamical system. It was shown how experimentally feasible physical constraints could be imposed to reduce the original four-dimensional system to one with the relative familiarity of planar dynamics. The concept of perfect thermokinetic matching was applied to this reduced system, which gave an explicit solution that was shown to define bounds for the state variables over a certain parameter range. For the unconstrained Endex system, however, global *dynamical* information is almost impossible to obtain. This is generally true of most complex dynamical systems dependent on many parameters. The classical technique for studying the time-evolution of dynamical systems is that of phase-space analysis, in which trajectories, stable and unstable manifolds, and separatrices in the space of the state variables (the phase space) for various initial conditions are deduced or plotted numerically. However, phase space analysis, and its extension, sensitivity analysis, have severe limitations with regard to the global study of thermokinetic systems. This is because initial conditions are usually prescribed, either by practical expedience or by virtue of being built into the model; and also because thermokinetic systems are typically constrained by at least several variable parameters, so that it is nearly impossible to obtain a qualitative portrait of the system dynamics over the physical, or even practicable, parameter realm by means of phase space analysis alone.

In this paper we turn to the steady-state analysis of the Endex system. Bifurcation theory, and its extension singularity theory, will play a central role in this study. The theory and techniques of degenerate bifurcation or singularity theory were developed by Guckenheimer & Holmes (1983) and Golubitsky & Schaeffer (1985), and applied to thermokinetic systems by Gray & Roberts (1988) and Ball (1999), among others. A major aim of this work is to show how the steady-state analyses required in the implementation of bifurcation theory provide qualitative insight into the causes of thermal instability that is not obtainable by other methods.

The scope of bifurcation theory: dynamical information from steady-state analysis.

The behaviour of solutions to the dynamical system 1 is the general problem of interest.

$$\begin{aligned}\frac{d\bar{v}}{dt} &= \bar{G}(\bar{v}, \bar{\lambda}) \\ \bar{v}_{(t=0)} &= \bar{v}(0).\end{aligned}\tag{1}$$

This is a concise representation of a coupled system of first-order, autonomous, ordinary differential equations, where \bar{G} is a vector of real-valued functions of the components of \bar{v} , the vector of state variables, and $\bar{\lambda}$, the vector of parameters. In the thermokinetic context of this work the physical quantities represented by the components of the state vector \bar{v} are species concentrations and temperatures, while the vector $\bar{\lambda}$ consists of time-invariant parameters such as the ambient conditions and thermal properties.

A dynamical process that is subject to mass or energy flux through the boundaries may attain a nonequilibrium steady state. Setting the left-hand side of equation 1 to zero

allows solution in terms of a single state variable v , and the steady states of equation 1 may be expressed as a scalar algebraic equation:

$$G(v, \bar{\lambda}) = 0. \quad (2)$$

Bifurcation theory is concerned with the study of the qualitative properties of solutions to equation 2. Specifically, the provenance of bifurcation theory is the *multiplicity*, *stability*, and *parameter dependence* of solutions to the problem (2). Multiplicity refers to the number of solutions to (2) at any given $\bar{\lambda}$. To define criteria for stability we need to refer back to the dynamical system (1), since the notion of stability involves assessing the effects of arbitrarily small, transient perturbations to the steady state. A steady-state solution is said to be asymptotically stable if a perturbation decays to zero as $t \rightarrow \infty$. Hirsch & Smale (1974) give precise criteria for stability: a solution to (2) is locally stable if the eigenvalues of the Jacobian matrix of (1) evaluated at the solution have nonpositive real parts, and is unstable otherwise.

One of the great strengths of the CSTR, both as a mathematical model and as a chemical conversion device, is the existence in it of non-trivial steady states. Much of what we know about time-dependent behaviour in thermokinetic systems actually comes from steady-state bifurcation analysis. Two instances of how steady-state analysis has enhanced our understanding of dynamical phenomena were described in Ball & Gray (1995): the critical damping condition, which marked the appearance of spiral trajectories in the phase plane; and the thermal runaway curve which, although based on a system-specific and strictly dynamical criterion, records the consequence of perturbations to the steady state. Another example comes from combustion theory, where the dynamical phenomenon of ignition is most successfully explained when the capacity for multiplicity is built into the model (Yang & Gray (1969)).

The use of steady-state analysis to extract information about dynamical processes is closely tied to the concept of quasi-static variation of parameters. Bifurcation diagrams, in which a system variable in the steady state is plotted as a function of a parameter (and which sometimes include other useful information such as indications of stability and the amplitude maxima of limit cycles), are often interpreted as portraits of the states of a system that is subjected either to deliberate “slow” parameter tuning or affected by incidental parameter drift.

Figure 1 illustrates one possible start-up procedure for coaxing the simulated example Endex CSTR from Part I, in which the reactions 2,3-epoxy-1-propanol \rightarrow 1,2,3-propanetriol and 2,3-dichloro-1-propanol \rightarrow 2,3-epoxy-1-chloropropane are thermally coupled, to a desired steady state of operation. For reference the dimensionless adiabatic Endex equations are:

$$\frac{dx_1}{d\tau} = -x_1 e^{-1/u_1} + f(1 - x_1) \quad (3)$$

$$\varepsilon_1 \frac{du_1}{d\tau} = x_1 e^{-1/u_1} + f\varepsilon_1(u_f - u_1) - l_{ex}(u_1 - u_2) \quad (4)$$

$$\frac{dx_2}{d\tau} = -x_2 \nu e^{-\mu/u_2} + f(1 - x_2) \quad (5)$$

$$\gamma\varepsilon_2 \frac{du_2}{d\tau} = -\gamma\alpha x_2 \nu e^{-\mu/u_2} + \gamma\varepsilon_2 f(u_f - u_2) + l_{ex}(u_1 - u_2) \quad (6)$$

(*Note:* The symbols and notation are defined at the end of the paper.)

[Figure 1 about here.]

The substance that reacts exothermally (2,3-epoxy-1-propanol) is titrated into the feed stream to one compartment of the reactor in contiguous doses, while the coupled compartment houses the endothermal reaction. Directly after each dose there is a transient spike which decays to a steady state, whereupon the next dose is added. The relatively large transients in the middle range of the dosage steps warn of possible rogue thermal behaviour, if the doses are too large. Conversely, it can be seen that, were the doses made smaller, the transients would become less of a problem. In the theoretical limit of *quasi-static* addition of the reactant the system is always at a steady state and the figure becomes a bifurcation diagram, with the reactant feed concentration replacing time on the horizontal axis. (*Note:* The doses of exothermal reactant represent variations in the specific reaction enthalpy, $(-\Delta H_1) c_{1,f}$. This quantity is obtained as an independently variable parameter very simply; by defining $\beta = 1/\alpha$, multiplying equations 4 and 6 through by β , and redefining ε_1 , ε_2 , and l_{ex} accordingly.)

Curves and surfaces of limit points or other codimension 0 bifurcations also may be interpreted as plots of quasi-static variations of two or three parameters. The importance of bifurcation diagrams to steady-state analysis lies in their value as devices for understanding and predicting dynamical behaviour, rather than their curiosity value as objects to be collected, sorted, and named. This, then, is the rationale for the steady-state analysis of the Endex problem. It is not intended here to construct a catalogue of all of the bifurcation possibilities. We shall use steady-state bifurcation analysis to reinforce the concept of quasi-static parameter variation and to provide a qualitative appreciation of the relationship of the Endex to the single-reaction CSTR. This is still a formidable task, because the system is, in general, analytically intractable. The bifurcation analyses of the single CSTR in Ball & Gray (1995) and Ball (1999) and the constrained reductions of the current system in Part I provide the formal framework within which the largely numerical steady-state analyses in this paper are carried out.

2 The two-dimensional system

At this stage we shall return to the constrained planar system that was derived in Part I, with reaction exponents (m and n) equal to 1:

$$\frac{dx_1}{d\tau} = -x_1 e^{-1/u} + f(1 - x_1) \quad (3)$$

$$(\varepsilon_1 + \gamma\varepsilon_2) \frac{du}{d\tau} = x_1 e^{-1/u} - \gamma\alpha x_2 \nu e^{-\mu/u} + f(\varepsilon_1 + \gamma\varepsilon_2)(u_f - u) \quad (7)$$

$$\gamma\alpha x_2 = \gamma\alpha - (1 - x_1) - (\varepsilon_1 + \gamma\varepsilon_2)(u_f - u) \quad (8)$$

$$u(0) = u_f, \quad x_1(0) = 1, \quad x_2(0) = 1. \quad (9)$$

This system in two dynamical state variables may be derived from equations 3–6 by taking the limit $1/l_{ex} \rightarrow 0$, and making use of the fact that it is integrable to obtain an

algebraic equation for x_2 as a function of x_1 and u . It is simplest and most illustrative to begin by imposing the perfect matching conditions

$$\alpha = \mu = \nu = \gamma = 1 \quad (10)$$

on equations 3–8 then proceed by relaxing the conditions $\alpha = 1$, $\mu = 1$ in turn, while retaining the other two conditions in equation 10, $\gamma = 1$, $\nu = 1$.

Thermal mismatching

The parameter α , the ratio of specific reaction enthalpies, describes the degree of thermal mismatching of the reactions. In terms of the Endex concept, the practicable range of this parameter is from zero ($c_{2,f} = 0$ and/or $\Delta H_2 = 0$) through 1 (perfect thermal matching) to possibly around 1.5 or 2, above which the the extent of endothermal cooling would probably quench the reactions. Global stability can be guaranteed for kinetically matched reactions where $\alpha \geq 1$, as the results of Part I showed, so our interest here is focused on the case where $\alpha < 1$. The steady-state bifurcation equation, with $\mu = \nu = \gamma = 1$ and for convenience $\varepsilon = \varepsilon_1 + \varepsilon_2$, can be written as a perturbation of that for the single-reaction adiabatic CSTR:

$$G = \frac{f e^{-1/u_s}}{e^{-1/u_s} + f} (1 - \alpha) + f \varepsilon (u_f - u_s) = 0. \quad (11)$$

The treatment of singularities in this system follows the analysis of the adiabatic CSTR in Ball (1999). The parametric equations for the curves of limit point bifurcations are given by

$$\begin{aligned} u_f &= u_s \left(1 - \frac{2u_s}{1 \pm \sqrt{1 - 4\varepsilon u_s^2 / (1 - \alpha)}} \right) \\ f &= \frac{(1 - \alpha) e^{-1/u_s}}{2\varepsilon u_s^2} \left[1 - 2\varepsilon u_s^2 \pm \sqrt{1 - 4\varepsilon u_s^2 / (1 - \alpha)} \right]. \end{aligned} \quad (12)$$

The conditions for the hysteresis bifurcation,

$$G = G_u = G_{uu} = 0, G_{uuu} \neq 0, \quad (13)$$

yield the coordinates of the cusp of the limit point curves:

$$\begin{aligned} u_s &= \frac{1}{2} \sqrt{\frac{1 - \alpha}{\varepsilon + 1 - \alpha}} \\ f &= e^{-2\sqrt{1 + \varepsilon / (1 - \alpha)}} \frac{(\sqrt{\varepsilon + 1 - \alpha} + \sqrt{1 - \alpha})}{(\sqrt{\varepsilon + 1 - \alpha} - \sqrt{1 - \alpha})} \\ u_f &= \frac{1}{2 \left(1 + \sqrt{\varepsilon / (1 - \alpha)} + 1 \right)}. \end{aligned} \quad (14)$$

All of these reduce to the corresponding equations of the single-reaction CSTR when $\alpha = 0$ (no endothermal effect). It would seem that this version of the Endex CSTR is qualitatively identical to the single reaction adiabatic CSTR, because no new degeneracies of multiplicity are introduced. However, in two-variable systems there is the

possibility of oscillatory instabilities arising from the Hopf bifurcation. To what extent is there an inbuilt potential for thermal oscillations in the kinetically matched planar Endex scheme? It is easily shown that this system cannot show Hopf bifurcations. The Jacobian matrix can be written

$$J = \begin{bmatrix} -e^{-1/u_s} - f & -x_s e^{-1/u_s} / u_s^2 \\ 0 & e^{-1/u_s} ((\alpha - 1) - \varepsilon (u_f - u_s)) / \varepsilon u_s^2 - e^{-1/u_s} - f \end{bmatrix}. \quad (15)$$

The Hopf bifurcation condition $\text{tr } J = 0$ gives an expression for u_f that can be positive:

$$u_f = u_s + \frac{\alpha - 1}{\varepsilon} + 2u_s^2 (1 + f e^{1/u_s}),$$

but the non-degeneracy condition $\det J > 0$ is violated:

$$\det J = - \left(e^{-\frac{1}{u}} + f \right)^2.$$

This is a negative quantity for all f and independent of α and ε .

Several saddle-node curves of the kinetically matched 2-dimensional Endex system are displayed in figure 2.

[Figure 2 about here.]

(Note that each of these curves is a transection at a selected value of ε of the respective limit-point shell.) From this figure and the above analysis it can be seen that the parameter α does not change the *qualitative* picture of multiplicity, because no new degeneracies are introduced. Physically we can see why this is so: the quantity represented by α can be regarded merely as a factor which generalizes the combined thermal properties of the reaction mixtures, to account for heat released or absorbed by the second reaction. In this sense it is not a “new” parameter, but a component of the the third dimension of the parameter space. Indeed, for the kinetically matched 2-dimensional Endex system, one can define the parameter $q = \varepsilon / (1 - \alpha)$ and the qualitative steady-state equivalence between this and the single-reaction adiabatic CSTR follows immediately.

Mismatched activation energies

Kinetic matching of endothermal and exothermal reaction partners is much more difficult to achieve experimentally than thermal matching. Activation energies are usually not regarded as being experimentally tunable; and even if, through ingenious experimentation with varieties and amounts of catalysts, kinetic matching of an Endex reaction pair were achieved to within a few percent, it is still a fact that thermal gradients are exponentially dependent on activation energies but only linearly dependent on specific reaction enthalpies. A reaction with a typical activation energy of 100kJ/mol at 300K proceeds at more than twice the rate of a reaction with $E = 98\text{kJ/mol}$ and fifty times

the rate of a reaction with $E = 90\text{kJ/mol}$, all other things being equal. Reactions which differ in activation energy by only a few percent may not “see” each other because they occur on quite different time-scales, and the efficaciousness of endothermal stabilization then is much diminished or non-existent. Where the activation energies are of comparable magnitude, but not identical, it is reasonable to expect to find bifurcations that may introduce thermal instabilities. A previous analysis of a thermokinetic system containing two Arrhenius terms (Gray & Forbes (1994)) showed a great diversity of phase portraits and bifurcation diagrams, due to both a dissipative term and unmatched reaction rates. By numerical analysis we can find no evidence of degeneration with respect to multiplicity in the current system. However, Hopf bifurcations can be introduced where $\mu \neq 1$, which contrasts strikingly with their absence where $\alpha \neq 1$. Figure 3 shows a numerically computed curve of saddle-node bifurcations, for $\mu = 1.06$, with an associated curve of Hopf bifurcations that terminates at a double zero eigenvalue (DZE) point.

[Figure 3 about here.]

The short branches of limit cycles emanating from these Hopf bifurcations are unstable, of low amplitude, and terminate at homoclinic orbits.

The numerical calculations indicate that the origin of the Hopf curve may be a DZE–DZE bifurcation at a point on the saddle-node curve. Computationally it is impossible to follow the fate of the Hopf curve accurately enough find such a point because the curve is extremely sensitive to parameter variations. Note that the DZE–DZE bifurcation is of codimension 2, whereas the highest order singularity of multiplicity in the steady states of equations 3–8 evidently is the hysteresis variety, of codimension 1. If the Hopf curve does originate at a codimension 2 singularity then it would seem that parameters which may not introduce degeneracies of multiplicity, because they are qualitatively already accounted for, may nevertheless introduce degeneracies of the Hopf bifurcation. We shall have the opportunity to observe further consequences of Hopf bifurcations in the Endex CSTR in the next sections. It is interesting to note that Hopf bifurcations and hence periodic solutions which occur here, do so in an adiabatic system.

3 Finite heat exchange in the unmatched adiabatic Endex CSTR

In this section, the parameter space of the unconstrained adiabatic Endex CSTR, equations 3–6, is investigated numerically. (*Note:* Since it is an integrable system, equations 3–6 may be regarded as having three dynamical variables and one algebraic variable, hence the phase space is effectively three-dimensional.) We are interested in how the combination of finite heat exchange between reactor compartments and imperfect reaction matching may affect patterns of multiplicity and Hopf bifurcations.

The efficiency of thermal exchange between endothermal and exothermal reactions is one of the more pressing questions arising from Part I and the previous section, where a conservative system in two dynamical variables was obtained by assuming a technological *fait accompli* of “perfect” thermal exchange. However, imperfect heat exchange could have serious design and operational implications. Even the best heat exchange surfaces

can undergo gradual occlusion during operation of a reactor, so it is wise to be prepared for the situation where u_1 and u_2 are not identical; i.e., where l_{ex} is finite.

Figure 4 shows numerically computed loci of saddle node and Hopf bifurcations in the f - u_f plane for four values of ε . It can be seen that the adiabatic Endex system displays the multiplicity patterns of *both* the adiabatic and the dissipative single reaction CSTR systems.

[Figure 4 about here.]

In passing from A to D we are moving along the “thermal properties” axis; which although geometrically named $\varepsilon = \varepsilon_1 + \gamma\varepsilon_2$, includes qualitatively and physically the quantities described by the groups α and μ . We may imagine replacing reaction mixtures of high overall heat capacity and/or low exothermal effect in A successively with mixtures of lower overall heat capacity and/or higher exothermal effect in B - D . (*Note:* For computational tractability in constructing these diagrams and those of Figure 7 below, it has been assumed that $\gamma = 1$ and $\varepsilon_1 = \varepsilon_2$.)

A scan of figure 4 shows the apparent upper island of multiplicity in A to be nothing more mysterious than a bulge on the limit point shell of which A - D are transections. The island—or bulge—represents the effect of thermal exchange on the intrinsic “thermal properties” multiplicity, the lower region of A . In B we note the appearance of the *transcritical* point. (The defining conditions for the isola and transcritical bifurcations are the same; they differ only in the sign of the non-degeneracy condition $G_{ff} \neq 0$ in the direction of approach—see Gray & Roberts (1988).) The transcritical point arises (or degenerates) via an *asymmetric cusp*; a codimension 2 bifurcation with the defining and non-degeneracy conditions

$$G = G_v = G_f = G_{ff} = 0; G_{vv} \neq 0, G_{fff} \neq 0. \quad (16)$$

(*Note:* Here G is a bifurcation function in the state variable v , which may denote either u_1 or u_2 , and the subscripts specify n th order differentiation with respect to v or f as appropriate.) The asymmetric cusp has not been found analytically or numerically but its effect can be seen in B : the lower hysteresis point of the upper island becomes tilted in the direction of the lower region of multiplicity. In C the hysteresis point of this lower region and the lower hysteresis point of the upper island have converged via a third codimension 2 bifurcation.

In B , the Hopf bifurcations associated with the lower region of multiplicity are due to kinetic mismatching; we encountered them earlier in figure 3. By contrast, the Hopf bifurcations to stable limit cycles associated with the upper region of multiplicity are due solely to a finite rate of heat exchange between the reactions. These separate loci begin to interact in C and unite in D . At some point there is also a switch in stability of the unstable limit cycles emanating from the lower Hopf bifurcations, because in D the entire locus is stable. The nature of the degeneration of the Hopf loci is therefore unclear, although a DZE-DZE bifurcation is one obvious possibility.

It is important to remember that the reactor described by equations 3–6 has *no* dissipative losses. The assumption that a dissipative term is necessary for oscillatory behaviour to occur, implicit in much of the CSTR literature, is incorrect. Limit cycle

behaviour is not due to a loss term *per se*, but may occur in an adiabatic system of two or more dimensions whenever there is competition between different rate processes. As with the single-reaction dissipative CSTR, limit cycles in the adiabatic Endex CSTR are associated with Hopf bifurcations and with multiplicity via homoclinic termini. We should also be aware of the possible occurrence in the Endex system of dynamical instabilities such as spiral trajectories and “wrong-way” behaviour.

From this and the previous discussions we may conclude that the cast of multiplicity has an intrinsic “thermal properties” component, associated with the thermal and energy properties of the reaction mixtures, and an “exchange” component, that moves into the parameter space from infinity. Oscillatory behaviour may be due to kinetic mismatching or imperfect thermal exchange, or interaction between the two.

4 Relaxation of enthalpy conservation

Thus far in the steady state analysis we have retained the conservation conditions

$$f_1 = f_2 \equiv f \quad \text{and} \quad l_d = 0 \quad (17)$$

on the Endex CSTR, firstly because this achieves a reduction of the state space dimensionality, and secondly because adiabatic operation allows the maximum recovery of heat, and thus possibly optimum conversion. However, quite apart from the fact that the conditions (17) represent idealizations, there may be legitimate control reasons for relaxing one or both of them. For example, it was shown in Ball (1999) that heat dissipation allows multiplicity to be avoided in the single diabatic CSTR by increasing the residence time and/or lowering the feed temperature, in a way that is impossible under adiabatic conditions. From the above discussion of multiplicity in the adiabatic Endex CSTR it might be fairly predicted that the cast of multiplicity in the truly dissipative system will be a distortion of that found in the single dissipative CSTR. A sneak preview of figure 7 confirms this impression, but we may wish to know more about particular causes and effects of dissipation. To what extent is the adiabatic ideal a workable (or unworkable) approximation? What is the role of the two feed flowrates in dissipative behaviour? How and where are oscillatory or other thermal instabilities introduced? The analysis of this section is based on the following dissipative system:

$$\frac{dx_1}{d\tau} = -x_1 e^{-1/u_1} + f_1 (1 - x_1) \quad (18)$$

$$\varepsilon_1 \frac{du_1}{d\tau} = x_1 e^{-1/u_1} + f_1 \varepsilon_1 (u_f - u_1) - l_{ex} (u_1 - u_2) \quad (19)$$

$$\frac{dx_2}{d\tau} = -x_2 \nu e^{-\mu/u_2} + f_2 (1 - x_2) \quad (20)$$

$$\gamma \varepsilon_2 \frac{du_2}{d\tau} = -\gamma \alpha x_2 \nu e^{-\mu/u_2} + (\gamma \varepsilon_2 f_2 + l_d) (u_f - u_2) + l_{ex} (u_1 - u_2). \quad (21)$$

The effects of independently variable residence times

Chemical reactors in industry often have two or more feedstreams, although relevant literature references to chemical reactor models that incorporate more more than one

flowrate or residence time are very scanty. Li (1994) demonstrated that a winged cusp singularity is introduced into a model for an isothermal autocatalytic reaction in a CSTR with two inflows of reactants; but there was no intimation that this singularity might be allowed through the breaking of a conservation condition. Of the two conservation conditions in (17) it is the first over which the experimenter has the greater degree of operational control. It is therefore of great practical interest to observe how two independent flowrates may affect the steady states.

There is also a theoretical reason why we are interested in uncoupling the residence times. In Ball (1999), evidence was presented that indicated a correspondence between the number of *physically different* quantities in a system and the highest codimension of degeneracy in the mathematical model. For the dissipative single CSTR it was found that it is not the separate feed and coolant temperatures *per se* that increased the codimension of system degeneracy, but rather the (implied) existence of finite coupling between the two temperature parameters. For the adiabatic Endex CSTR it was found that the thermal and energy properties of the second reaction are already accounted for in the “energy” or thermal properties dimension of the parameter space, in the sense that they do not introduce higher degeneracies of multiplicity. The flowrates (inverse residence times) f_1 and f_2 —like the feed and coolant temperatures—are physically identical and independently variable quantities, yet we saw in Part I that they make or break a conservation condition. How, then, do the residence times affect the structure of the parameter space?

For simplicity, we shall use the assumption of perfect thermal exchange and retain the second conservation condition in (17), so that the effect of f_2 may be observed without interference from l_{ex} and l_d . The steady-state bifurcation equation can be written as:

$$G = \frac{f_1 e^{-1/u_s}}{e^{-1/u_s} + f_1} - \frac{\gamma \alpha f_2 \nu e^{-\mu/u_s}}{\nu e^{-\mu/u_s} + f_2} + (f_1 \varepsilon_1 + f_2 \gamma \varepsilon_2) (u_f - u_s) = 0. \quad (22)$$

A suitable strategy in principle might be to search for limit, hysteresis, pitchfork bifurcations, and so on, by writing down the appropriate derivatives, then compare the codimension of the highest order singularity with that of the fully conservative Endex system. However, by inspection we can see that the higher order derivatives with respect to u_s will be sufficiently complex to thwart such attempts at analytic solution. Instead, we shall impose the additional condition $\alpha = 0$. (Admittedly, this is a rather absurd condition, for it means that no reaction or no thermal effect at all is occurring in the endothermal compartment. This situation is contrary to the philosophy of the Endex concept; but it has pedagogical value.) Then, with the bifurcation equation

$$G = \frac{f_1 e^{-1/u_s}}{e^{-1/u_s} + f_1} + \varepsilon (f_1 + f_2) (u_f - u_s) \quad (23)$$

(where for convenience only, $\gamma \varepsilon_2 = \varepsilon_1 = \varepsilon$) the following results are obtained:

1. From the defining conditions for the winged cusp

$$G = G_u = G_f = G_{fu} = G_{uu} = 0; G_{uuu} < 0, G_{ff} < 0 \quad (24)$$

the single winged cusp point W is unphysical:

$$W = (u_s, u_f, \varepsilon, f_1, f_2) = (-1/2, \infty, 0, \infty, 0). \quad (25)$$

2. We may expect the winged cusp to occur in the physical region for zero- or finitely-coupled feed temperatures, u_{f_1} and u_{f_2} . For zero-coupled feed temperatures the bifurcation equation becomes

$$G = \frac{f_1 e^{-1/u_s}}{e^{-1/u_s} + f_1} + \varepsilon f_1 (u_{f_1} - u_s) + \varepsilon f_2 (u_{f_2} - u_s).$$

The algebra yields the following equations for the coordinates of the winged cusp, at fixed u_{f_2} :

$$\begin{aligned} u_s &= \frac{2u_{f,2}}{1 - 4u_{f,2}} \\ u_{f_1} &= \frac{u_s(1 + u_s)}{1 + 2u_s} \\ f_1 &= e^{-1/u_s} \left(\frac{1 + 2u_s}{1 - 2u_s} \right) \\ \varepsilon &= \frac{(1 - 4u_s^2)(1 - 2u_s)}{4u_s^2} \\ f_2 &= 2u_s e^{-1/u_s} \frac{(1 + 2u_s)}{(1 - 2u_s)^2}. \end{aligned} \quad (26)$$

3. The pitchfork singularity, of codimension 2, is the highest order degeneracy in the system where u_{f_1} and u_{f_2} are infinitely coupled, as in equation 23. The defining conditions

$$G = G_u = G_{uu} = G_f = 0; G_{uuu}G_{fu} \neq 0 \quad (27)$$

yield the following parametric equations for the pitchfork locus:

$$\begin{aligned} u_f &= \frac{u_s}{1 + 2u_s} \\ f_1 &= e^{-1/u_s} \left(\frac{1 + 2u_s}{1 - 2u_s} \right) \\ \varepsilon &= \frac{(1 - 4u_s^2)(1 - 2u_s)}{8u_s^2} \\ f_2 &= e^{-1/u_s} \left(\frac{1 + 2u_s}{1 - 2u_s} \right)^2. \end{aligned} \quad (28)$$

4. This tells us that, contrary to expectations, the uncoupling of f_1 and f_2 does introduce singularities of higher codimension. The highest order singularity in the corresponding fully conservative system is, from above, the hysteresis variety, of codimension 1.

5. Thus we may suspect that there is a rather elusive connection between conservation conditions, state space dimensionality, and the codimension of the highest order singularity in a bifurcation problem. Although *formally* the parameters f_1 and f_2 describe the same physical property (mass flux), their uncoupling *effectively* introduces a physical property that is *qualitatively equivalent* to heat loss. Figure 5 displays a limit point shell from equation 23 for a fixed value of f_2 . It is formally identical to that of the single-reaction dissipative CSTR in Ball (1999).

[Figure 5 about here.]

Returning now to the bifurcation equation (22) it can be seen that in general we may expect to find a variety of codimension 1, 2, and 3 singularities in this system. Can we hope (or hope *not*) to find higher order singularities? This is an open question because, as mentioned above, the higher order derivatives with respect to u_s become very complex. Since we have just demonstrated the qualitative equivalence of heat exchange, heat loss, and a second residence time it appears unlikely that higher order bifurcations are hidden in the system, because there are no more physically independent properties to vary.

These results also indicate that we should expect to find the usual assortment of Hopf bifurcations, degeneracies, and other oscillatory instabilities in the Endex CSTR with variable residence times. This expectation is borne out in figure 6, which is a bifurcation diagram for an Endex system under the conditions indicated by equation 23. It shows a branch of limit cycles emanating from the upper Hopf bifurcation and ending at a homoclinic terminus. (There is also a branch of limit cycles from the lower Hopf bifurcation that ends at a homoclinic terminus. It is so short that it does not show on the diagram.) The Hopf bifurcations have occurred solely as a result of uncoupling the residence times. Engineers should note that under these circumstances attempts to control reactant conversion by manipulating the feed flow rates separately may induce thermal oscillations.

[Figure 6 about here.]

This concludes the discussion of the enthalpy flux conservation condition.

Heat losses

The effects of relaxing the second conservation condition in (17) should be simpler to assess, because l_d appears linearly in the bifurcation equation. In this section we shall look at how heat losses affect multiplicity in equations 18–21 with $f_1 = f_2 \equiv f$. The structure of the parameter space may be deduced from the sequence of limit-point shell transections in figure 7, which have been constructed at fixed values of l_{ex} and l_d .

[Figure 7 about here.]

They should be compared to those in figure 4. Again, as in figure 4, in passing from A to D we are moving backwards along the ε -axis. The unexpected appearance of *two* islands of multiplicity in A is mundanely resolved as we move back to lower values of ε : they are nothing more than transections of knobbles on a surface of multiplicity that

begins to resemble the limit-point shell of the single diabatic CSTR. Some of the possible features of this surface, inferred from Figure 7 and from the previous discussion of the unconstrained adiabatic system, may be enumerated:

1. There may be *two* pitchfork points. The upper pitchfork is associated with finite heat exchange. It moves in from infinity as l_{ex} is *decreased*. The lower pitchfork is associated with finite heat loss, and it moves out from zero as l_d is *increased*.
2. The upper and the lower pitchforks may each degenerate to a winged cusp on variation of a fourth parameter—but there is a physical condition for this. It was shown in Ball (1999) that the occurrence of the winged cusp in the single CSTR requires a looser parameter space, in the sense that feed and coolant temperatures must be finitely coupled. In the dissipative Endex CSTR the association of the lower pitchfork with heat losses suggests that the winged cusp of the lower pitchfork may occur for zero- or finitely-coupled feed and coolant temperatures. The association of the upper pitchfork with heat exchange suggests that an upper winged cusp requires two zero- or finitely-coupled feed temperatures. (*Note:* This does not imply that the two hypothesized winged cusps must coexist.)
3. The possibility of bifurcations of codimension > 3 must be countenanced, although the evidence indicates that l_{ex} , l_d , and f_2 are different incarnations of an overall “loss quantity”, which forms the fourth dimension of the parameter space, just as the combined “intrinsic energy properties” were found to form the third dimension of the parameter space. If this is true, then we may expect these and any other qualitatively similar parameters to introduce smooth bumps and hollows on the limit point surface due to codimension 2 bifurcations, but not necessarily cause bifurcations of higher order.

5 Example

Finally, we turn to a specific example. We shall observe the steady states of the example Endex reactor described in Part I, which was last seen in the time-series/bifurcation diagram of figure 1 of this paper. Recall also that the phase portrait of figure 7A of Part I showed that dynamical stabilization of the exothermal reaction could be achieved under idealized 2-dimensional conditions at specified operating parameter values. In general we cannot expect to see stabilization under all operating conditions, so we must aim for a range of steady states that are thermally resilient yet maximise conversion of both reactants. A parameter plane diagram of saddle-node and Hopf bifurcations for the example pair of reactions housed in an adiabatic Endex reactor is shown in figure 8A, while in figure 8B the thermokinetic parameters have been manipulated to eliminate multiplicity and Hopf bifurcations in the lower range of f .

[Figure 8 about here.]

The bifurcation diagrams in Figure 9 have been reconstructed from figure 8B at a selected value of f by calculating the steady states and the Hopf branches from the Hopf

bifurcation point to as close to the homoclinic terminus as possible. The diagrams indicate the possibilities for optimization, with respect to conversion and temperatures. (For easy reference we have provided dimensional temperature units on the axes.) It can be seen by comparison of figures 8 and 9 that multiplicity at low flowrates is built in to the system by virtue of the mismatch in rates—but it should be noted that it is *low-temperature* multiplicity. Clearly there is potential here for using the hysteresis loop as a form of control or switch. However, it may be a one-way switch as indicated by the arrows: we may jump the system to a safe high-conversion state by adjusting the feed temperature upwards, but a branch of limit cycles may be an impediment to the reverse procedure of quenching the reactions. Paradoxically, it is the branch of limit cycles in the thermokinetically matched system in figure 9*D*, *E*, and *F* that is more dangerous because the stable attractor can occur above the boiling point, whereas in the unmatched system of *A*, *B*, and *C* the branch is unstable and contained well below the boiling point. We see that in this case a certain degree of kinetic mismatching actually tempers the oscillations indicated by figures 8*B* and 9*D*, *E*, and *F* that are purely exchange in origin.

[Figure 9 about here.]

Conclusion

The Endex reactor is a promising new development in chemical reactor design and engineering technology. In Part I we showed that unequivocal dynamical stabilization could be achieved in a two-reaction Endex CSTR over a wide range of thermokinetic parameters. In this paper we applied a combination of degenerate bifurcation theory and numerical analysis to the steady states of this system and achieved a comprehensive survey of the parameter space. What seemed at first to be a hopelessly large and intractable system, in terms of the number of parameters and variables, became somewhat simpler when the bifurcation analysis showed that the parameters fall into only four physically distinct groups, representing *ambient temperature*, *mass flux*, *intrinsic thermal and energy properties*, and *heat losses*.

The bifurcation structure of the Endex parameter space was found to be a smooth perturbation of the single-reaction CSTR parameter space, with distortions of the saddle-node bifurcation surface, or limit-point shell, occurring via additional codimension 2 bifurcations. Mismatched reaction rates and dissipative terms introduce Hopf bifurcations, which may be a potential source of thermal instability in reactors with poorly matched reaction pairs, different flowrates through the compartments, inadequate heat exchange surfaces, or badly chosen heat dissipation rates. We used an example reaction couple, hydration of 2,3-epoxy-1-propanol and dehydrochlorination of 2,3-dichloro-1-propanol, to demonstrate the value of steady-state analysis in reactor design and operation. It was shown how the concept of quasi-static parameter variation could be usefully applied to assess a dynamical procedure such as start-up or shut-down. Bifurcation diagrams were used to compare the behaviour of the selected reaction pair with the matched ideal.

This study is restricted to reactors of the CSTR configuration, although preliminary work indicates no particular difficulties in extending the Endex concept to other configurations such as tubular, batch, or semi-batch reactors. In future work we shall report

on the results of these studies, as well as applications of the concept to reactor and storage-tank situations where there may be large spatial gradients.

Notation and Definitions

Dimensional quantities

A = frequency factor in units consistent with the reaction exponents m and n .

c = concentration of reactant (mol l^{-1})

\bar{C} = weighted volumetric specific heat capacity of feed mixture ($\text{J l}^{-1}\text{K}^{-1}$)

E = activation energy (J mol^{-1})

F = feed flowrate (l s^{-1})

ΔH = reaction enthalpy (J mol^{-1})

L = combined heat transfer coefficient ($\text{Js}^{-1}\text{K}^{-1}$)

m, n = reaction rate exponents

R = gas constant ($8.314\text{J mol}^{-1}\text{K}^{-1}$)

t = time (s)

T = temperature (K)

V = reaction mixture volume (l)

Dimensionless groups

(Notes: 1. Although the dimensionless groups are defined in terms of the above dimensional quantities, any convenient but consistent set of units may be used when it is necessary to recover a dimensional quantity. For example, if it is more convenient to use the mass of the reaction mixture rather than the volume, then concentration would be measured in units of mol kg^{-1} , specific heat capacity in units of $\text{J kg}^{-1}\text{K}^{-1}$, and mass flowrate in kg s^{-1} would be used. 2. Subscripts 1, 2, d , ex are appended as appropriate to the dimensionless groups, and to the dimensional quantities that are not already subscripted as part of the definitions.)

$$f = F/V A_1 c_{1,f}^{n-1}$$

$$l = LE_1/V_1 A_1 c_{1,f}^n (-\Delta H_1) R$$

$$u = RT/E$$

$$x = c/c_f$$

$$\alpha = \Delta H_2 c_{2,f} / (-\Delta H_1) c_{1,f}$$

$$\gamma = V_2/V_1$$

$$\varepsilon = \overline{C}E_1/c_{1,f} (-\Delta H_1) R$$

$$\mu = E_2/E_1$$

$$\nu = A_2c_{2,f}^{m-1}/A_1c_{1,f}^{n-1}$$

$$\tau = tA_1c_{1,f}^{n-1}$$

Other symbols

$$q = \varepsilon/(1 - \alpha)$$

v = a state variable

W = winged cusp bifurcation

G = a bifurcation function

$$\beta = 1/\alpha$$

θ = dimensionless scaling factor (0.0338)

Subscripts

1 = of the exothermal reaction, of the reactor compartment housing the exothermal reaction

2 = of the endothermal reaction, of the reactor compartment housing the endothermal reaction

a = ambient, of the surroundings

d = dissipative, of heat transfer to the surroundings

ex = exchange, of heat transfer between reactions

f = of the feed

s = of the steady state

Abbreviations

DZE = double zero eigenvalue

trJ = trace of the Jacobian matrix of differential coefficients of the linearization of coupled ODEs.

$\det J$ = determinant of the Jacobian matrix of differential coefficients of the linearization of coupled ODEs.

Endnote

For computing the the data in figures 1, 3, 4, 6, 7, 8, and 9, the equations were scaled by the factor $e^{1/\theta}$, where θ is a reference temperature selected only for computational convenience. Thus the exponential term is written as $e^{-1/\theta} e^{1/\theta} e^{-1/u_1} = e^{-1/\theta} e^{1/\theta - 1/u_1}$, then dividing through by $e^{-1/\theta}$ also scales the dimensionless time, flowrates, and loss and exchange coefficients. Scaling the equations in this way forestalls possible numerical problems, and avoids having very small numbers ($\sim 10^{-10}$) on the axes of the diagrams.

Acknowledgments

The authors thank the Australian Research Council for support of this research.

The success of this work owes much to the computer programs that were used or adapted to produce the numerical and graphical output. For most of the bifurcation and parameter plane diagrams the Fortran program Auto (Doedel (1986)) was used in its (1994) version. This program has the wonderful ability to compute branches of periodic solutions and to compute second-parameter continuations at codimension zero bifurcations. It cannot, however, compute its own starting solutions. These were obtained from another excellent piece of public domain scientific software, the C program Dstool (Guckenheimer *et al.* (1993)), which also was used to compute trajectories for phase portraits (in Part I) and time series. The graphical capabilities of these packages are limited however, so that the diagrams using the the numerical output were rendered by the program Gnuplot (Williams & Kelley (1993)), with subsequent (and sometimes extensive) hand editing of the generated output of Postscript code. For some diagrams, the fast function-plotting capability of Gnuplot was also used. The bifurcation surfaces, and some two-dimensional plots of Part 1, were obtained using the commercial package Mathematica (Wolfram (1991)). Again, the realization of these plots required extensive post-translational modification of the generated Postscript code.

References

- Ball, R. (1999). The origins and limits of thermal steady-state multiplicity in the continuous stirred tank reactor. *Proc. R. Soc. Lond. A* **455**, 141–161.
- Ball, R & Gray, B.F. (1995). Transient thermal behaviour of the hydration of 2,3-epoxy-1-propanol in a continuously stirred tank reactor. *Ind. Eng. Chem. Res.* **34**, 3726–3736.
- Doedel, E. J. (1986). *AUTO: Software for Continuation and Bifurcation Problems in Ordinary Differential Equations*. Technical report, Californian Institute of Technology.
- Golubitsky, M. & Schaeffer, D.G. (1985). *Singularities and Groups in Bifurcation Theory*, volume 1. Springer–Verlag, New York.
- Gray, B. F. & Roberts, M. J. (1988). A method for the complete qualitative analysis of two coupled O.D.E.'s dependent on three parameters. *Proc. R. Soc. Lond. A* **416**, 351–389.

- Gray, B.F. & Ball, R. (1999). Thermal stabilization of chemical reactors. I. The mathematical description of the Endex reactor. *Proc. R. Soc. Lond. A* **455**, 163–182.
- Gray, B.F. & Forbes, L.K. (1994). Analysis of chemical kinetic systems over the entire parameter space IV. The Sal’nikov oscillator with two temperature-dependent reaction rates. *Proc. R. Soc. Lond. A* **443**, 621–642.
- Guckenheimer, J. & Holmes, P. (1983). Non-linear Oscillations, Dynamical Systems and Bifurcations of Vector Fields. In *Appl. Math. Sciences*, volume 42, New York. Springer Verlag.
- Guckenheimer, J., Myers, M.R, Wicklin, F.J. & Worfolk, P.A. (1993). *Dstool—a dynamical systems analysis and exploration toolkit*. Center for Applied Mathematics, Cornell University.
- Hirsch, M.W. & Smale, S. (1974). *Differential Equations, Dynamical Systems, and Linear Algebra*. Academic Press, New York.
- Li, Ru-Sheng (1994). Continuous flow stirred tank reactor with two inflows of reactants: A versatile tool for study of bifurcation in chemical systems. *Chem. Eng. Sci.* **49**, 2029–31.
- Williams, T. & Kelley, C. (1993). *Gnuplot—an interactive plotting program*. Copyright (C) 1986–1993 Thomas Williams, Colin Kelley.
- Wolfram, S. (1991). *Mathematica: a system for doing mathematics by computer*. Addison-Wesley, Redwood City, California, second edition.
- Yang, C. H. & Gray, B. F. (1969). Unified theory of explosions, cool flames, and two-stage ignitions. *Trans. Faraday Soc.* **65**, 1614–1622.

List of Figures

1	<p>Quasi-static parameter variation in the adiabatic Endex CSTR. <i>A</i>: Time series simulating quasi-steady-state addition of exothermal reactant to feedstream. Initial conditions at $t = 0$: $x_1(0) = 0$, $x_2(0) = 1$, $T_1(0) = T_2(0) = 291\text{K}$; thereafter the initial conditions are equal to the steady state values of the variables. $\beta = 1/\alpha$ is increased in steps: 0, 0.2, 0.4, 0.5, 0.7, 0.9, 1.1, 1.3, 1.5, 1.7. <i>B</i>: In the limit of quasi-static increments in β the time-series maps to a bifurcation diagram. Dimensionless values of the parameters: $u_f = 0.033$, $f = 3.04$, $\varepsilon_1 = 39.1 = \gamma\varepsilon_2$, $\nu = 0.047$, $\mu = 0.968$, $l_{ex} = 800$, $\theta = 0.0338$ (see endnote).</p>	20
2	<p>Saddle-node curves of the kinetically matched 2-dimensional Endex system. $\varepsilon = 0.25$ (no scaling factor is used here).</p>	21
3	<p>Saddle-node (solid) and Hopf (dashed) curves for the 2-dimensional Endex model with kinetic mismatching. $\mu = 1.06$, $\alpha = \nu = 1$, $\varepsilon_1 = 50 = \gamma\varepsilon_2$, $\theta = 0.0338$ (see endnote). The Hopf bifurcations are to unstable limit cycles. <i>DZE</i> = double zero eigenvalue point.</p>	22
4	<p>Saddle-node (solid) and Hopf (dashed) curves for the 3-dimensional adiabatic Endex CSTR. Parameters: $\alpha = \gamma = \nu = 1$, $\mu = 1.05$, $l_{ex} = 50000$, $\theta = 0.0338$ (see endnote).</p>	23
5	<p>A limit point shell from equation 23 for a fixed value of f_2.</p>	24
6	<p>A bifurcation diagram for a perfect-exchange Endex system in which the endothermal effect is zero and the enthalpy flux conservation condition is broken. Solid lines: stable steady states, dashed line: unstable steady states, dotted line: upper amplitude trace of limit cycle branch. Parameters: $\varepsilon_1 = \gamma\varepsilon_2 = 29.5$, $f_1 = 0.5$, $f_2 = 3$, $\alpha = 0$, $\nu = \mu = 1$, $l_d = 0$, $\theta = 0.0338$ (see endnote). <i>HB</i> = Hopf bifurcation.</p>	25
7	<p>A sequence of limit-point shell transections of the diabatic Endex CSTR. In all diagrams, $\alpha = \mu = \nu = 1$.</p>	26
8	<p><i>A</i>: Parameter plane diagram for the example reaction pair in an adiabatic Endex CSTR. $\varepsilon = 29.5$, $\alpha = 0.754$, $\nu = 0.047$, $\mu = 0.968$, $\theta = 0.0338$ (see endnote), $l_{ex} = 1000$. <i>B</i>: Parameter plane diagram for an ideal matched reaction pair in an adiabatic Endex CSTR. $\varepsilon = 29.5$, $\alpha = 1$, $\nu = 1$, $\mu = 1$, $l_{ex} = 1000$, $\theta = 0.0338$ (see endnote). Solid lines: saddle-node loci, dashed lines: Hopf loci.</p>	27
9	<p>Reconstructed bifurcation diagrams from Figure 8. <i>A</i>, <i>B</i>, and <i>C</i>: $\varepsilon = 29.5$, $\alpha = 0.754$, $\nu = 0.047$, $\mu = 0.968$, $l_{ex} = 1000$, $f = 2$, $\theta = 0.0338$ (see endnote). <i>D</i>, <i>E</i>, and <i>F</i>: $\varepsilon = 29.5$, $\alpha = 1$, $\nu = 1$, $\mu = 1$, $\theta = 0.0338$ (see endnote), $l_{ex} = 1000$, $f = 2$. Solid lines: stable branches, dashed lines: unstable branches, dotted lines: unstable limit cycle branch, dash-dot lines: stable limit cycle branch.</p>	28

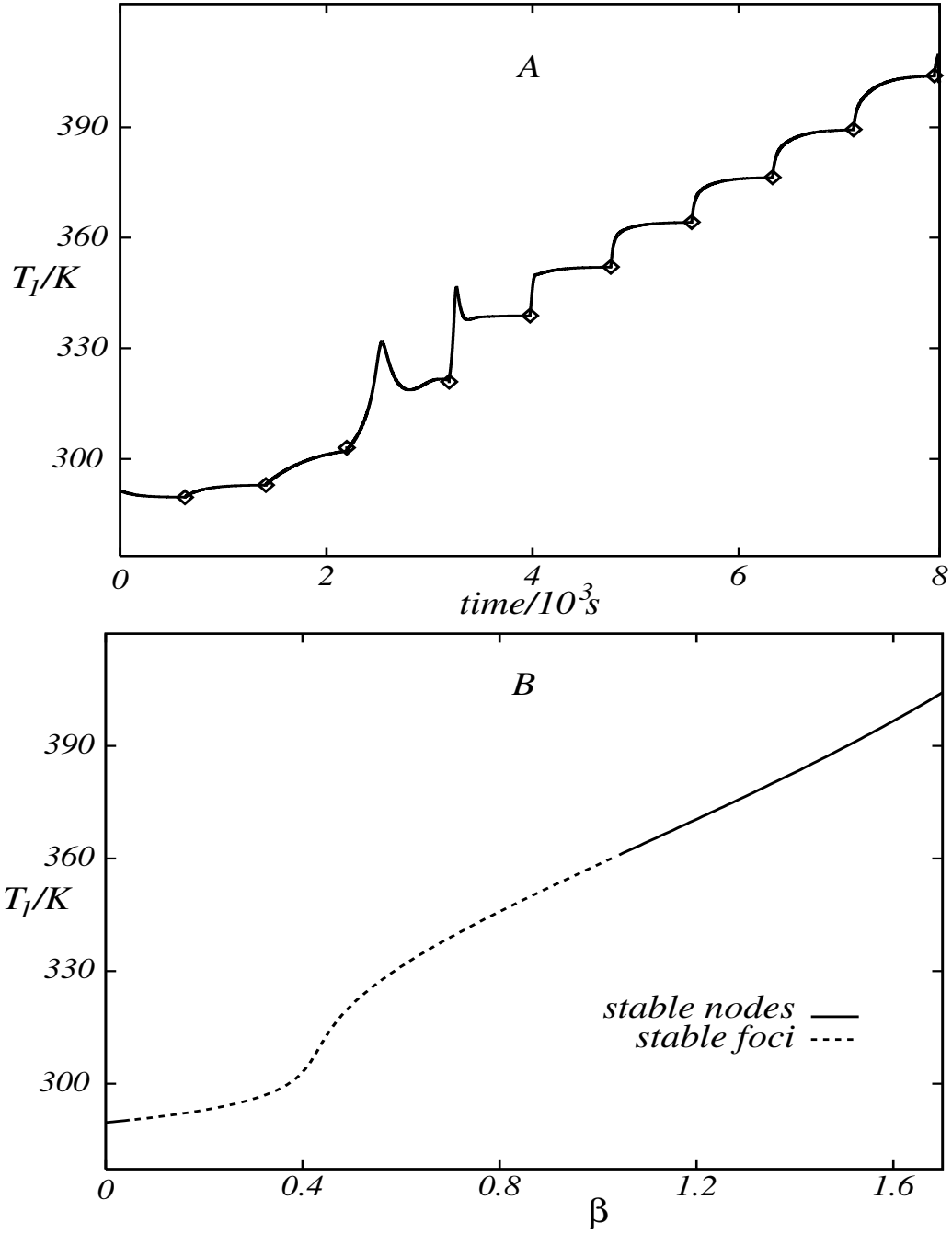


Figure 1:

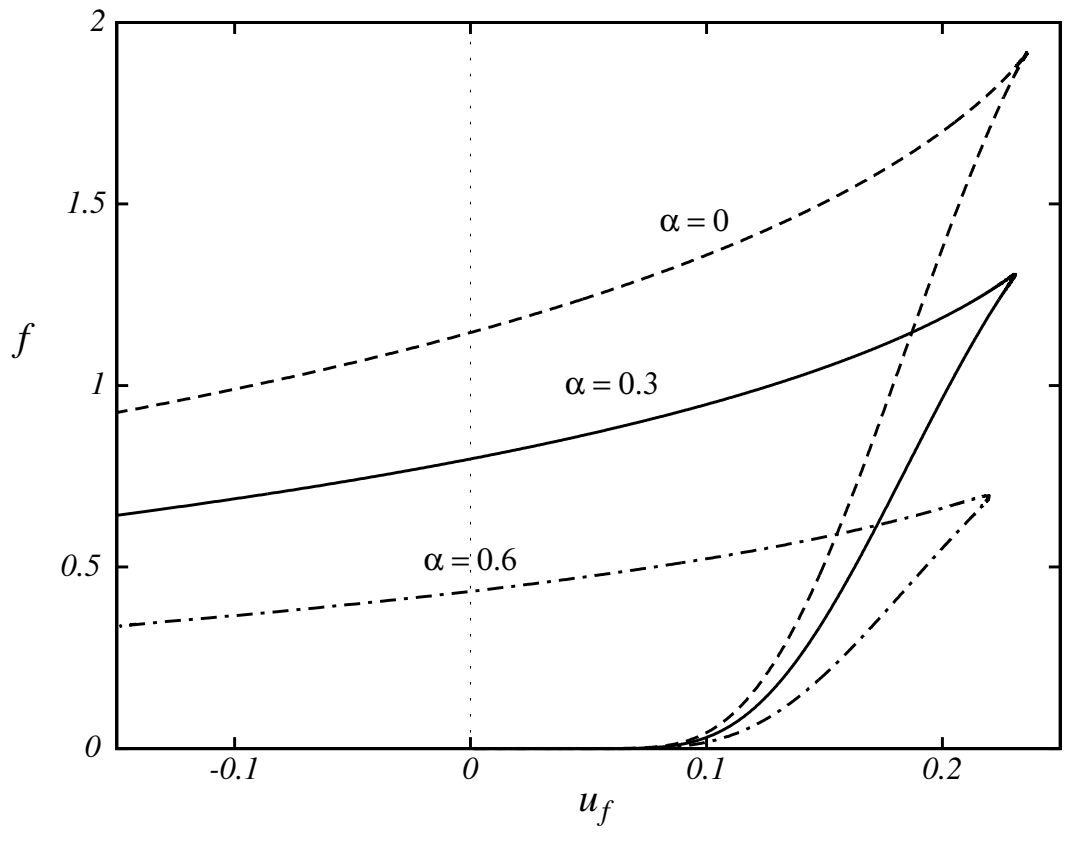


Figure 2:

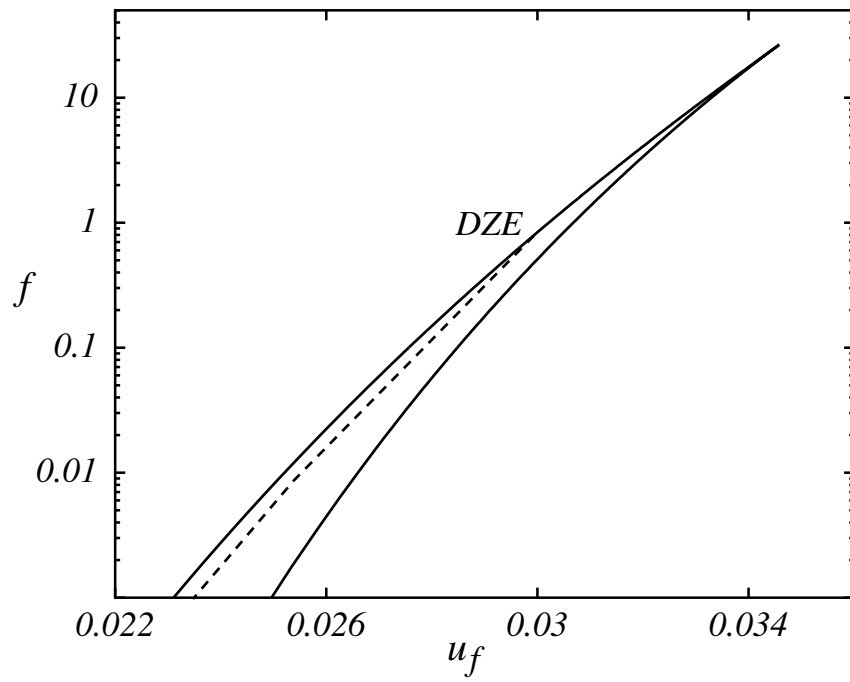


Figure 3:

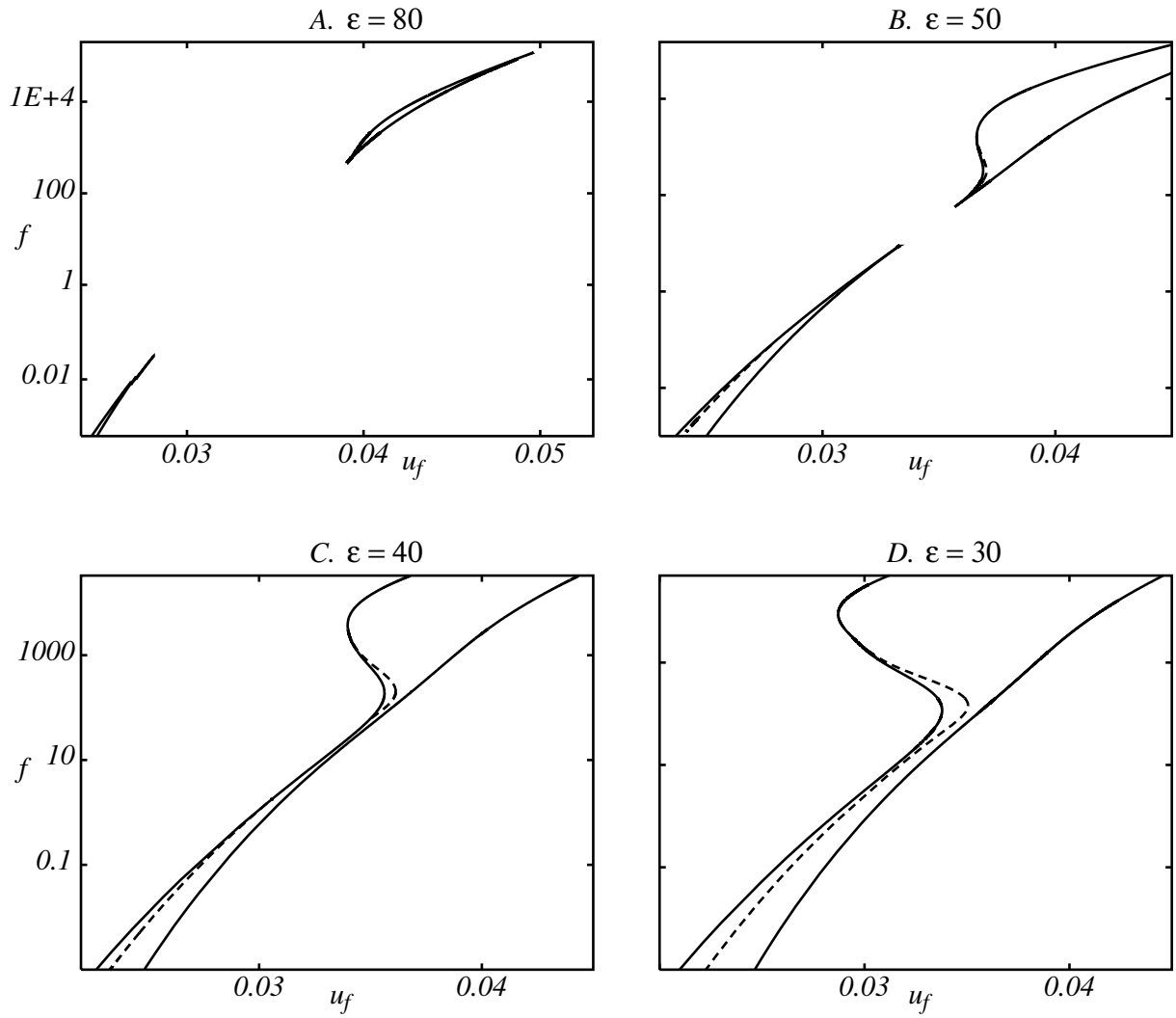


Figure 4:

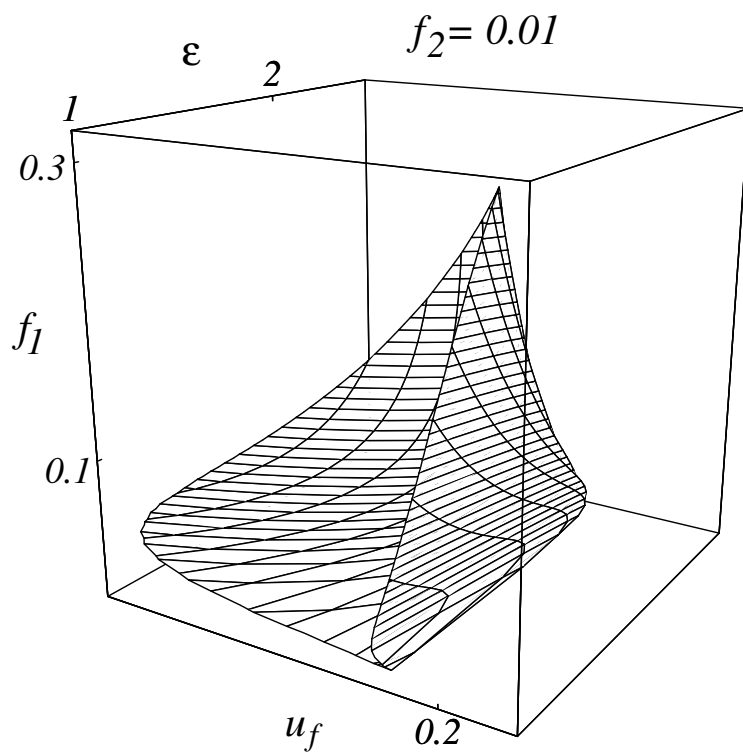


Figure 5:

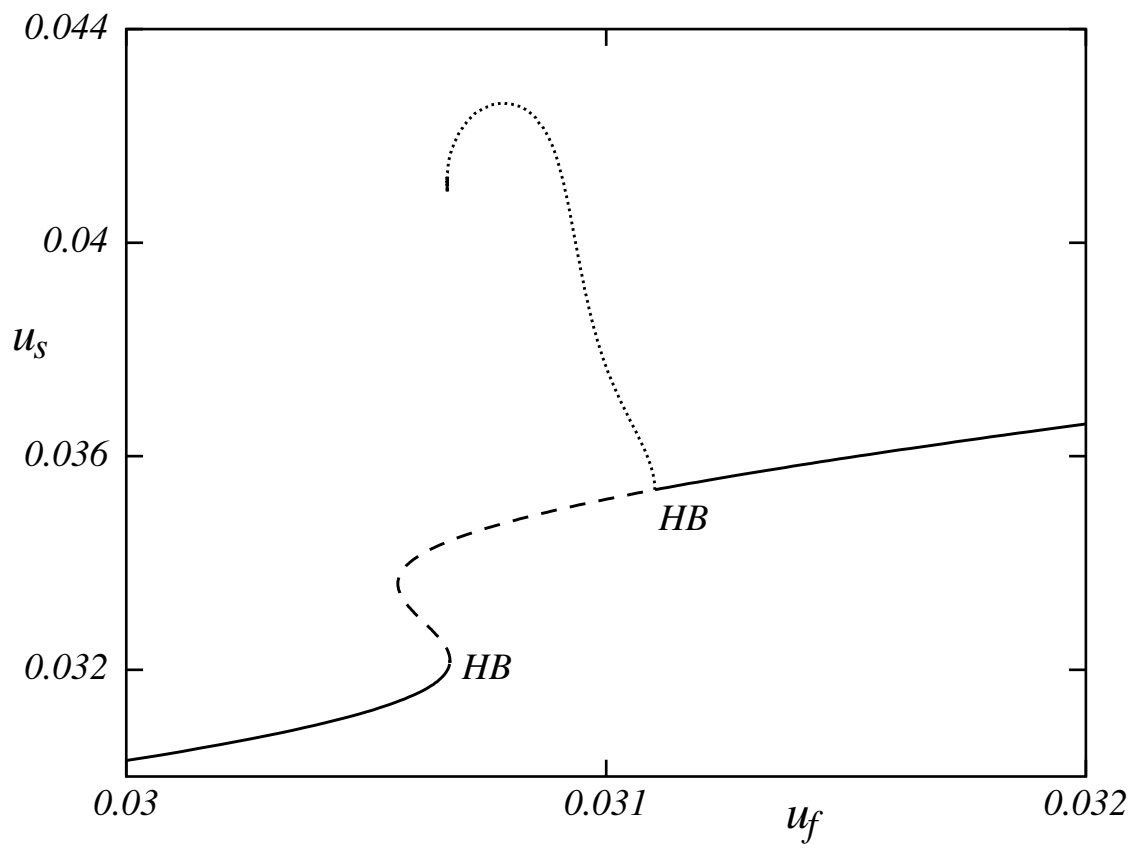


Figure 6:

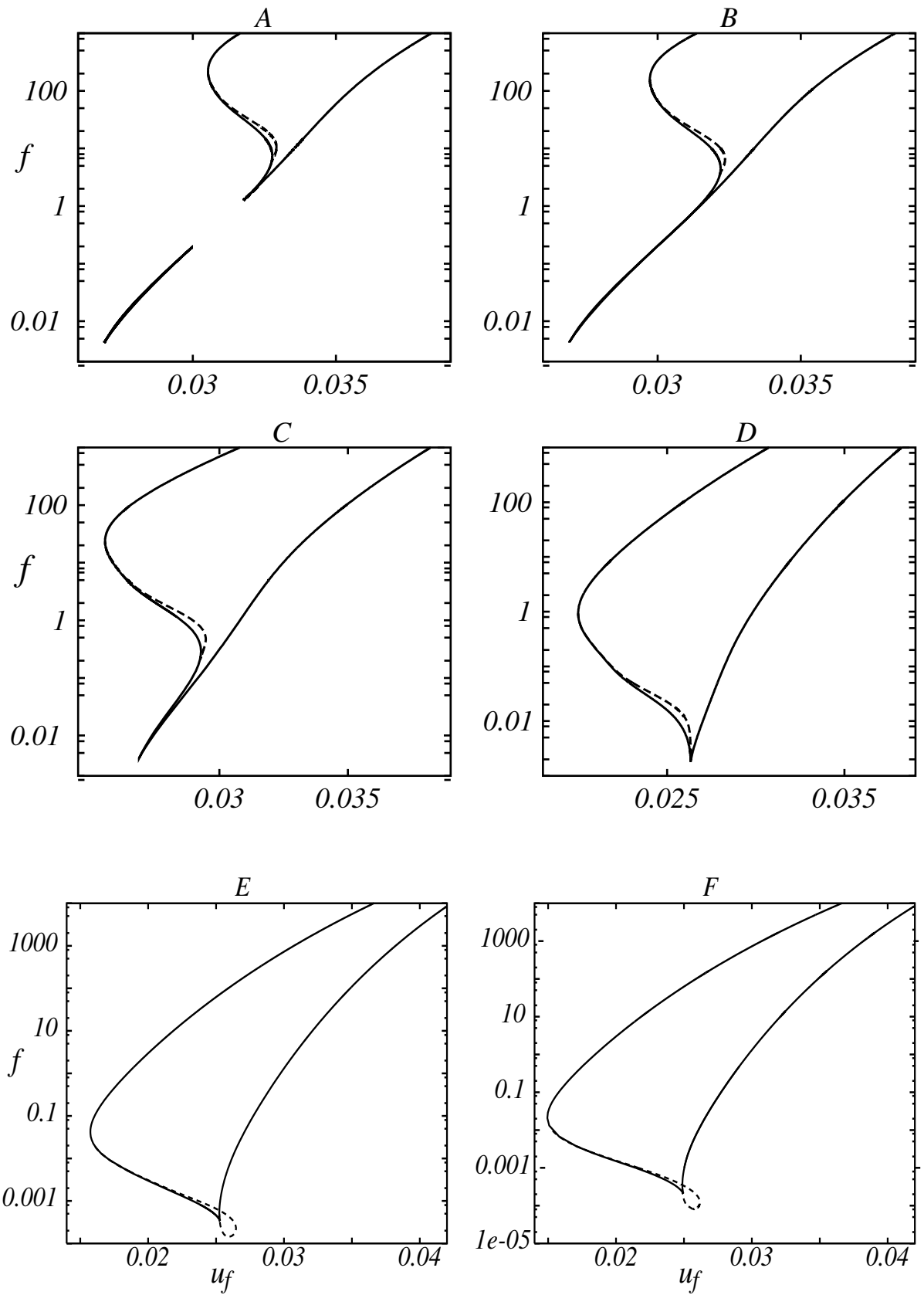


Figure 7:

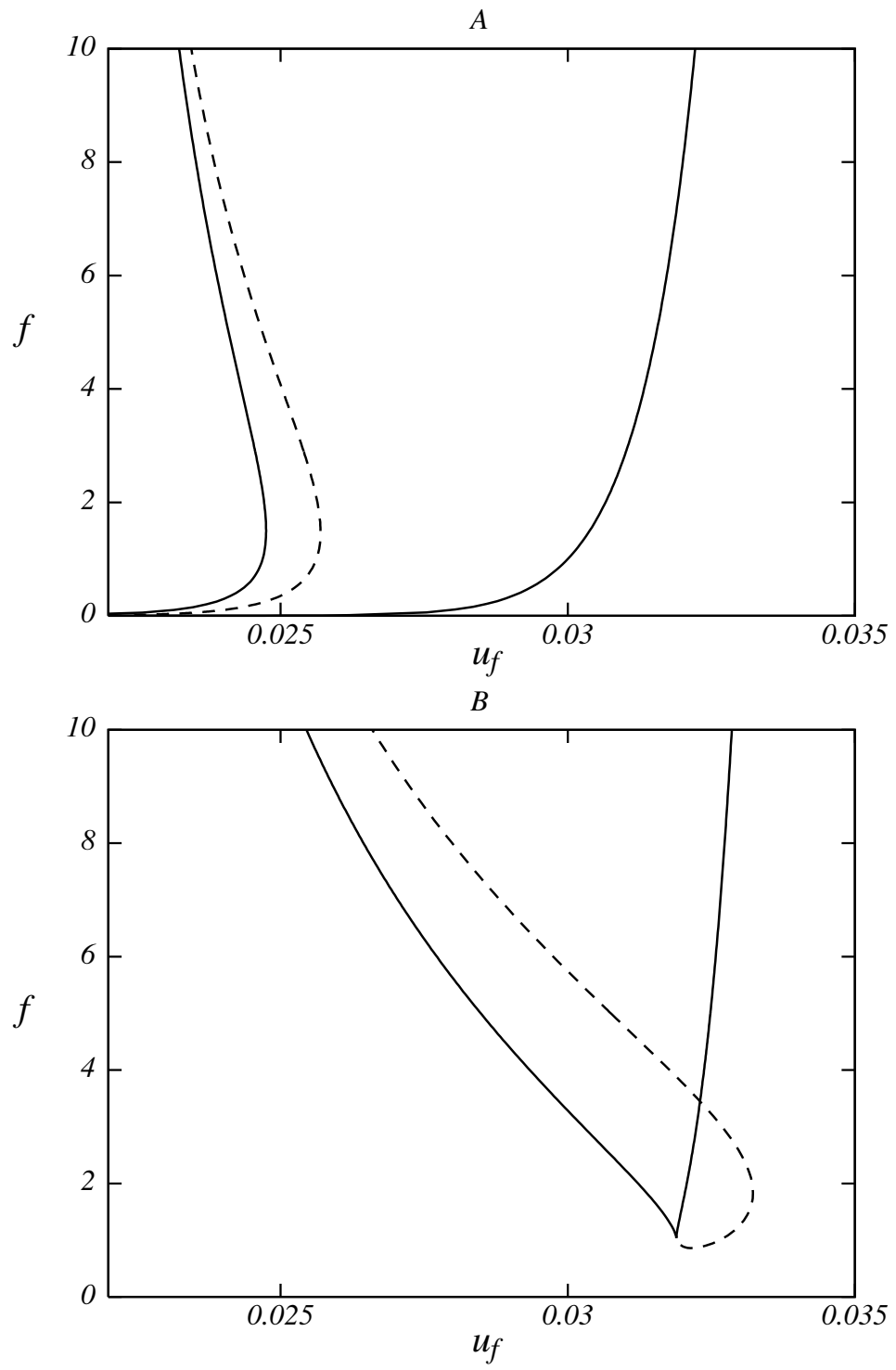


Figure 8:

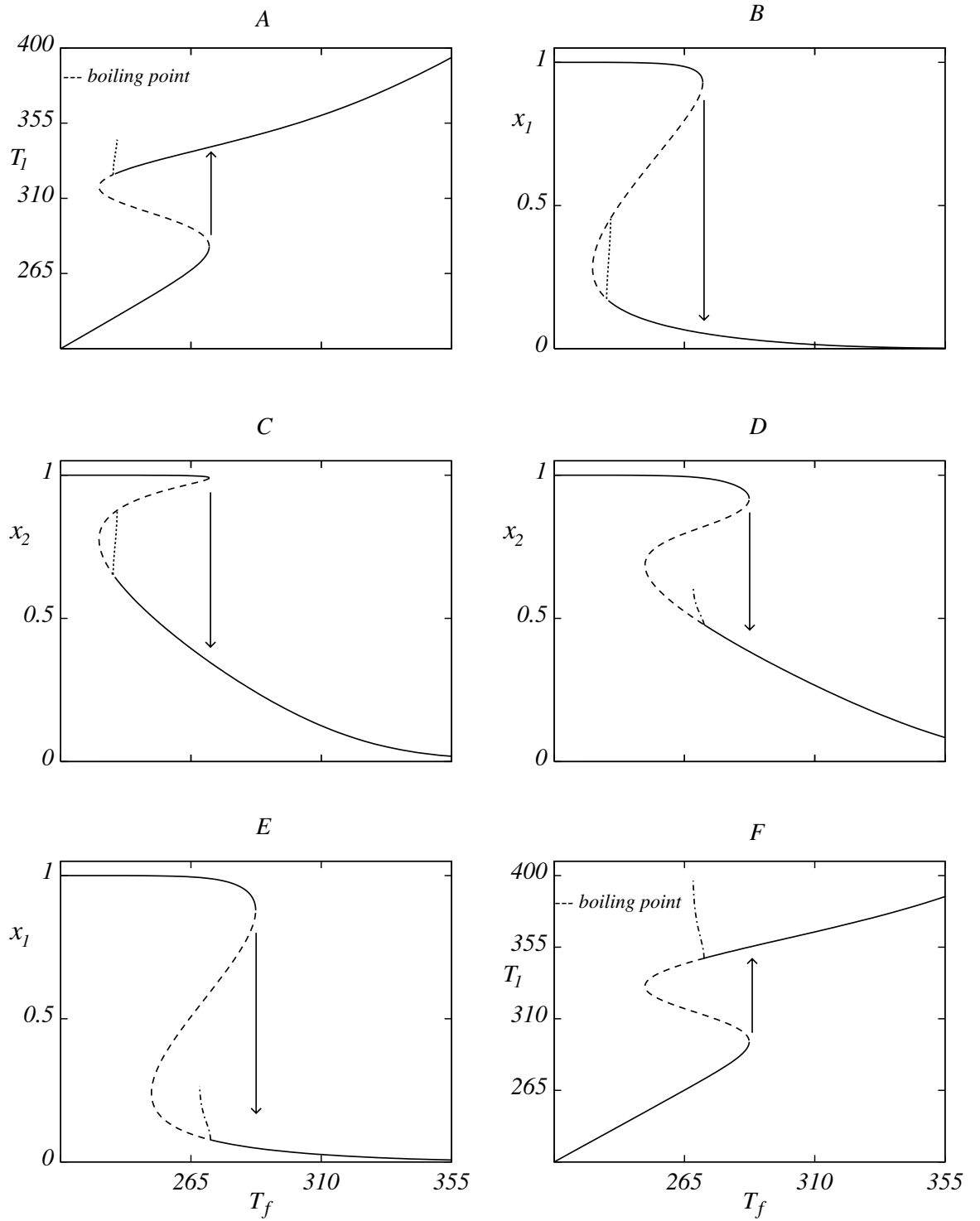


Figure 9: